Hindawi Publishing Corporation
Journal of Applied Mathematics
Volume 2012, Article ID 104952, 18 pages
doi:10.1155/2012/104952

*Research Article*

# Modeling Electromechanical Overcurrent Relays Using Singular Value Decomposition

**Feng-Jih Wu,[1] Chih-Ju Chou,[1] Ying Lu,[2] and Jarm-Long Chung[3]**

[1] *Department of Electrical Engineering, National Taipei University of Technology, Taipei 10608, Taiwan*
[2] *Department of Computer and Communication Engineering, St. John's University, Tamsui District, New Taipei City 25135, Taiwan*
[3] *Department of Power Supply, Taiwan Power Company, Zhongzheng District, Taipei City 10016, Taiwan*

Correspondence should be addressed to Feng-Jih Wu, roger@mail.sju.edu.tw

Received 17 August 2012; Accepted 5 November 2012

Academic Editor: Ricardo Perera



This paper presents a practical and effective novel approach to curve fit electromechanical (EM) overcurrent (OC) relay characteristics. Based on singular value decomposition (SVD), the curves are fitted with equation in state space under modal coordinates. The relationships between transfer function and Markov parameters are adopted in this research to represent the characteristic curves of EM OC relays. This study applies the proposed method to two EM OC relays: the GE IAC51 relay with moderately inverse-time characteristic and the ABB CO-8 relay with inverse-time characteristic. The maximum absolute values of errors of hundreds of sample points taken from four time dial settings (TDS) for each relay between the actual characteristic curves and the corresponding values from the curve-fitting equations are within the range of 10 milliseconds. Finally, this study compares the SVD with the adaptive network and fuzzy inference system (ANFIS) to demonstrate its accuracy and identification robustness.

## 1. Introduction

Power generation systems generally have few large generators connected directly to their subtransmission networks and distribution networks. Thus, the fault currents of buses do not differ much from those of transmission lines. This makes low-cost, reliable, and easily coordinated electromechanical (EM) overcurrent (OC) relays suitable for protection coordination relay in the subtransmission networks and distribution networks. Although some older relays have been replaced by new digital ones, there are still many EM OC relays in service.

The operation principle of the EM OC relay is to introduce an electric current into the coil of an electromagnet to produce eddy currents with phase differences. This in turn generates induction torque on the rotation disc of the relay. The proper contact closing time can be set by adjusting the distance between the fixed and the movable contacts, achieving protection coordination between upstream and downstream. However, due to the mechanical nature of the relay, there are inertial and frictional effects. Therefore, unlike a digital relay [1], it is not possible to describe the characteristic curve of an EM OC relay using a single precise equation. Manufacturer manuals generally provide families of characteristic curves with different time dial (TDS) values. These are all piecewise nonlinear continuous smooth descending curves.

Accurate representations of the inverse-time EM OC relay characteristics play an important role in the coordination of power network protection schemes. In the early days, researchers were interested in fitting EM OC relay characteristics curves [2] to facilitate protection coordination in conventional power systems. After the introduction of the digital OC relays, better curve-fitting of EM OC relay characteristic [3–6] is even more important for proper protection coordination. Most of the literature about curve fitting shows the absolute values of errors [7–9], while some show the averages of absolute values of errors [9, 10]. Only a few studies show the maximum absolute values of percentage errors [10], which are harder to curve fit, and no studies show the maximum absolute values of errors, which are the hardest to curve fit. For EM OC relays at small values of $M$ (multiples of tap value current), for example, 1.3–3.5, the relay operating time changes nonlinearly and drastically, and only one study [10] shows the curve fitting results in this range of $M$ values.

This paper applies the Hankel matrices and the singular value decomposition (SVD) [11–13] to obtain the curve-fitting equation of the characteristic curves of two EM OC relays under state space with modal coordinates [14, 15]. To demonstrate the accuracy of the curve-fitting results, the current study not only shows all the maximum absolute values of errors, maximum absolute values of percentage errors, average of absolute values of errors, and average of absolute values of percentage errors, but also considers smaller values of $M$ where the relay operating time changes nonlinearly and drastically. For even better accuracy, this paper reduces the maximum absolute values of errors to less than an alternating current cycle in the range of a few milliseconds (ms), as opposed to 3 cycles in [3] or 2 cycles in [8].

The paper proposed a new application algorithm to fit the characteristic curves of the EM OC relays, using one unified equation to represent their characteristics. Finally, this study uses the SVD method to fit the characteristic curves of EM OC relays. Comparing the results with those obtained by [9] demonstrates the accuracy and identification robustness of the SVD method.

The content of this paper is as follows: Section 2 introduces the representations for the characteristic curves of EM OC relays, the mathematical derivation of the curve fitting of the characteristic curves of the EM OC relays using SVD method is outlined in Section 3, two cases are studied in Section 4 to verify the approach, the performance of the SVD and the well-behaved ANFIS algorithm are compared in Section 5, and the conclusion is in Section 6.

## 2. Models of the Electromechanical (EM) Overcurrent (OC) Relay Characteristic

The characteristic of an EM OC relay is determined by its magnetic circuit design, and the manufacturers provide the characteristics in the relay manuals with curves in a two-dimensional plot with $M$ the abscissa and operating time the ordinate. Some typical models for the characteristic of an EM OC relay are as follows.

### 2.1. Exponential and Polynomial Forms

Various exponential and polynomial forms of equations are summarized and recommended by the IEEE Committee [3], for example, (2.1)–(2.5) below, for EM OC relay characteristic curve fitting. In some studies [7, 8, 10] that apply numerical methods to determine the best coefficients of the curve-fitting equations, the maximum absolute values of percentage errors are as large as 15% [10], so there is still much room for improvement. Consider

$$t = \frac{Y \times \mathrm{TDS}}{(M^p - 1)} + Z = \frac{Y \times \mathrm{TDS}}{\left((i/I_n)^p - 1\right)} + Z, \tag{2.1}$$

$$t = a_0 + a_1 \times \mathrm{TDS} + a_2 \times \mathrm{TDS}^2 + a_3 \times \mathrm{TDS}^3 + \cdots, \tag{2.2}$$

$$t = b_0 + \frac{b_1}{(M-1)} + \frac{b_2}{(M-1)^2} + \frac{b_3}{(M-1)^3} + \cdots, \tag{2.3}$$

$$t = c_0 + \frac{c_1}{\log M} + \frac{c_2}{(\log M)^2} + \frac{c_3}{(\log M)^3} + \cdots, \tag{2.4}$$

$$\begin{aligned} t = d_0 + d_1 \times \mathrm{TDS} &+ \frac{d_2 \times \mathrm{TDS}}{(M-1)^2} \\ &+ \frac{d_3 \times \mathrm{TDS}^2}{(M-1)} + \frac{d_4 \times \mathrm{TDS}^2}{(M-1)^2} \\ &+ \frac{d_5 \times \mathrm{TDS}}{(M-1)^3} + \frac{d_6 \times \mathrm{TDS}^2}{(M-1)^4}, \end{aligned} \tag{2.5}$$

$$t = \mathrm{TDS} \times \left(\frac{F}{(M^p - 1)} + G\right) + H, \tag{2.6}$$

where $t$: relay operating time. TDS: time dial setting. $i$: fault current on the secondary side of the CT. $I_n$: current tap setting. $M$: multiples of tap value current, $M = i/I_n$. $F$, $G$, $H$, $Y$, $Z$, $a_n$, $b_n$, $c_n$, $d_n$, $p$: constants.

### 2.2. Customized Characteristic Equation

A customized characteristic Equation (2.6) is obtained by modifying (1) in [16] for simulation. The IEEE normal standard inverse-time digital relay characteristic representation is obtained by letting $K = 0$ [5], and the IEC normal standard inverse-time digital relay characteristic representation is obtained by letting both $K = 0$ and $B = 0$ [17].

Take the characteristic curves of the ABB's EM OC relay CO-8 as an example [18]. The recommended values of $A$, $B$, $K$, and $p$ in (2.6) are 8.9341, 0.17966, 0.028, and 2.0938, respectively in [16]. Figure 1 shows the actual and the fitted characteristic curves with TDS settings of 0.5, 2, 5, and 10. The averages of absolute values of errors of the 488 sampling operating times for TDS settings 0.5, 2, 5, and 10 are 99.95, 189.18, 382.16, and 449.94 ms,

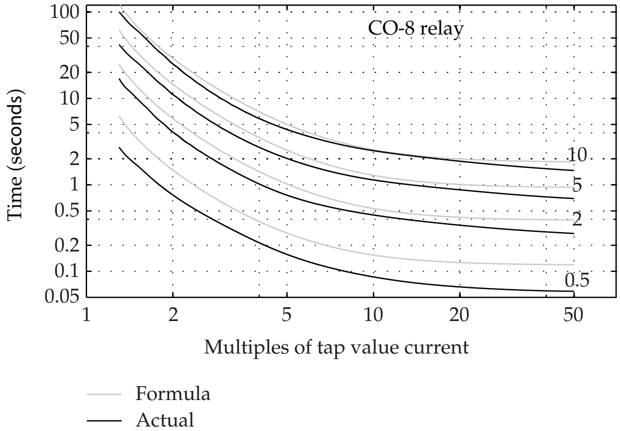


**Figure 1:** The actual characteristic curves and the curves fitted by (2.6) for the CO-8 relay.

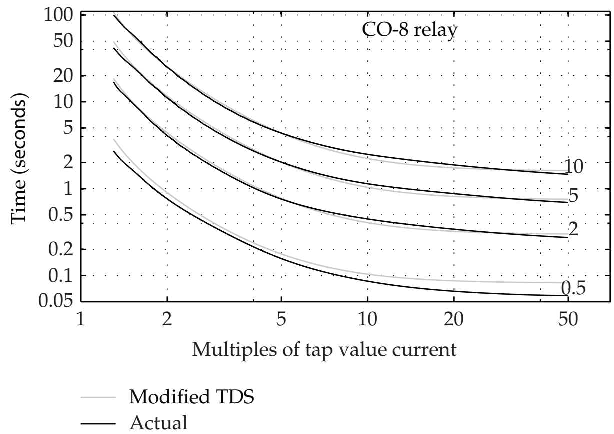


**Figure 2:** The actual characteristic curves and the modified curves fitted by (2.6) for the CO-8 relay.

respectively. The fitted curve differs considerably from the actual characteristic curve and cannot be used directly as a good replacement.

Consider the case [19] in which the TDS settings in (2.6) are modified to 0.3, 1.5, 4, and 8.7, while their manufacture data counterparts remain the same as 0.5, 2, 5, and 10, respectively (expressed as Figure 2). The averages of absolute values of errors of the four sets of 488 sampling operating times taken between the modified fitted curve and the actual characteristic curve are 28.64, 32.54, 90.97, and 168.74 ms, respectively. Although this modified (2.6) has better accuracy, it is still not good enough to represent the actual characteristic curves provided by the manufacturer.

## *2.3. Data Base Method*

The values of $M$ and the corresponding operating times are stored directly [3, 4]. This type of representation is commonly used today, but requires large data storage. Because the relay characteristics cannot be represented by an equation, interpolation method is usually applied to estimate data points not stored.

### *2.4. Artificial Intelligence Techniques*

Researchers are applying more artificial neural network and fuzzy model techniques [7, 9] to optimal curve fitting. Among these approaches, the ANFIS algorithm developed by Geethanjali and Slochanal [9] shows promising results.

## 3. The Singular Value Decomposition (SVD) Method

Based on the concept of transfer function, this paper proposes an algorithm to represent the characteristic curves of EM OC relays to calculate Markov parameters [20, 21]. After the Hankel matrices [20] are constructed, they are decomposed by SVD and transformed to state space system under modal coordinates. Finally, the state space solution is found, and the fitting equation is obtained by transformation back to the continuous $M$-domain system [21]. The proposed algorithm processes the $M$-domain data directly and is thus an identification method in the $M$-domain.

The SVD method is as follows [11–15, 20, 21].

*Step 1.* Find the estimated operating time $t_0$ on the EM OC relay characteristic curve corresponding to a specific multiple of tap value current $\overline{M}$ as in (3.1). Repeat this process to the right with incremental step $\Delta M$ to form the sample sequence $t_k$, $k = 1, 2, 3, \ldots$, where

$$\overline{M} = M_{\min} - \Delta M \tag{3.1}$$

$M_{\min}$: minimum multiple of tap value current. $\Delta M$: increment sampling step.

*Step 2.* Use $t_k$, $k = 1, 2, 3, \ldots$ to form the Hankel matrices $H(0)$ and $H(1)$ in (3.2) as follows:

$$H(0) = \begin{bmatrix} t_1 & t_2 & \cdots & t_h \\ t_2 & t_3 & \cdots & t_{h+1} \\ \vdots & \vdots & \ddots & \vdots \\ t_h & t_{h+1} & \cdots & t_{2h-1} \end{bmatrix}_{h\times h},$$
$$H(1) = \begin{bmatrix} t_2 & t_3 & \cdots & t_{h+1} \\ t_3 & t_4 & \cdots & t_{h+2} \\ \vdots & \vdots & \ddots & \vdots \\ t_{h+1} & t_{h+2} & \cdots & t_{2h} \end{bmatrix}_{h\times h}. \tag{3.2}$$

*Step 3.* Apply SVD to the Hankel matrix $H(0)$ to obtain matrices $R$, $\Sigma$, and $S$ in (3.3)

$$H(0) = R\Sigma S^T. \tag{3.3}$$

*Step 4.* Determine the proper dimension $n$ for the modal coordination system in (3.3) and obtain matrices $R_n$, $\Sigma_n$, and $S_n$ in (3.4), where $n$ is also the number of fitting waveform components and its range is form 1 to the rank of $\Sigma$

$$R\Sigma S^T = \begin{bmatrix} R_n & R_0 \end{bmatrix} \begin{bmatrix} \Sigma_n & \underline{0} \\ \underline{0} & \Sigma_0 \end{bmatrix} \begin{bmatrix} S_n^T \\ S_0^T \end{bmatrix}. \tag{3.4}$$

*Step 5.* Calculate the matrices $\widehat{A}$, $\widehat{B}$, and $\widehat{C}$, which are the estimates of the matrices $A$, $B$, and $C$ in the state space system (3.5), as (3.6) and (3.7) show

$$\begin{gathered} M(k+1) = AM(k) + Bu(k) \quad k = 0,1,2,\ldots, \\ t(k) = CM(k) + Du(k), \end{gathered} \tag{3.5}$$

$$\widehat{A} = (\Sigma_n)^{-1/2} R_n^T H(1) S_n (\Sigma_n)^{-1/2}, \tag{3.6}$$

$$\begin{gathered} \widehat{B} = (\Sigma_n)^{1/2} S_n^T E_1, \\ \widehat{C} = E_1^T R_n (\Sigma_n)^{1/2}, \end{gathered} \tag{3.7}$$

where $E_1^T$ is shown as (3.8)

$$E_1^T = \begin{bmatrix} 1 & 0 & \cdots & 0 \end{bmatrix} \tag{3.8}$$

and the system matrix $D$ is as shown in (3.9)

$$D = t_0. \tag{3.9}$$

*Step 6.* Transform the state space Equation (3.5) into modal coordinate system to find $\Lambda$, $B_m$, and $C_m$ as (3.10), (3.12), (3.13), and (3.14) show

$$\begin{gathered} M_m(k+1) = \Lambda M_m(k) + B_m u(k), \quad k = 0,1,2,\ldots, \\ t(k) = C_m M_{\mathrm{m}}(k) + Du(k), \end{gathered} \tag{3.10}$$

where $M_m(k)$ is as shown in (3.11)

$$M_m(k) = \Psi^{-1} x(k), \tag{3.11}$$

$$\Lambda = \Psi^{-1} \widehat{A} \Psi = \begin{bmatrix} \lambda_1 & & \underline{0} & \\ & \lambda_2 & & \\ & & \ddots & \\ & \underline{0} & & \lambda_n \end{bmatrix}, \tag{3.12}$$

$$B_m = \Psi^{-1} \widehat{B}, \tag{3.13}$$

$$C_m = \widehat{C} \Psi, \tag{3.14}$$

where $\lambda_i$: eigenvalues of $\widehat{A}$, $i = 1,2,\ldots,n$. $\Psi$: matrix whose columns are the eigenvectors of $\widehat{A}$.

*Step 7.* Obtain the unit impulse response sequence from (3.10), the state space equations under modal coordinates, as known system Markov parameters in (3.15) below:

$$
\begin{aligned}
t(k) &= t_0, \quad k = 0 \\
&= CA^{k-1}B = C_m \Lambda^{k-1} B_m \quad k = 1, 2, 3, \ldots \\
&= \sum_{i=1}^{n} c_i \lambda_i^{k-1} b_i
\end{aligned}
\tag{3.15}
$$

*Step 8.* Derive the equation of the fitted relay characteristic curve by transforming back to continuous $M$-domain system (3.16)

$$
\begin{aligned}
t(M) = {} & \sum_{i=1}^{n_1} C_i e^{-\alpha_i (M-\overline{M})} \\
& + 2\sum_{i=1}^{n_2} K_i A_{r_i}^{-f_i(M-\overline{M})} \cos\left(2\pi f_i \left(M - \overline{M}\right) + \varphi_i\right) \\
& + \sum_{i=(n_2+1)}^{n_3} K_i A_{r_i}^{-f_i(M-\overline{M})} \cos\left(2\pi f_i \left(M - \overline{M}\right) + \varphi_i\right),
\end{aligned}
\tag{3.16}
$$

where $t$ is the operating time with $M$ as its variable. $n_1$ is the number of the smooth waveform components. $n_2$ is the number of the paired oscillation waveform components (thus the coefficient 2). $n_3$ is the number of the independent oscillation components. $(n_3 - n_2)$ is the number of the unpaired oscillation waveform components. $C_i, \alpha_i, K_i$, and $A_{r_i}$ are the constants. $f_i$ is the oscillation frequency, in Hertz. $\varphi_i$ is the oscillation phase shift, in radian.

Equation (3.17) describes the relationship among $n$, $n_1$, $n_2$, and $n_3$

$$
n = n_1 + 2n_2 + (n_3 - n_2) = n_1 + n_2 + n_3. \tag{3.17}
$$

The characteristic curves of an EM OC relay can be represented by a digital state space model, and the desired bound of the maximum absolute value of errors may be established by selecting an appropriate system model order $n$. Equation (3.16) is an unified equation by SVD method to fit EM OC relays characteristic curves, all of which are piecewise nonlinear continuous smooth descending curves. Any of such characteristic curves can be fitted by simply changing the values of the parameters in the equation.

## 4. Cases Study

The following case study involves two EM OC relays: the GE moderately inverse-time relay IAC51 [22] and the ABB inverse-time relay CO-8 [18]. To be both accurate and reasonable, the constraint set for the fit is that the maximum absolute value of errors between all the fitted sampling points and the actual characteristic curves for each TDS be less than 10 milliseconds. The calculations in this study were made using MATLAB.

**Table 1:** The 26 parameters in (4.1) for the IAC51 relay.

| TDS | 1 | 4 | 7 | 10 |
|---|---|---|---|---|
| $n$ | 4 | 9 | 12 | 13 |
| $C_1$ | $4.7488E-01$ | $1.7515E+00$ | $3.4807E+00$ | $5.6144E+00$ |
| $\alpha_1$ | $2.4356E+00$ | $3.5435E+00$ | $3.5331E+00$ | $3.5255E+00$ |
| $C_2$ | $3.3871E-01$ | $1.7317E+00$ | $3.4524E+00$ | $5.1574E+00$ |
| $\alpha_2$ | $5.9703E-01$ | $9.9106E-01$ | $9.5370E-01$ | $9.6362E-01$ |
| $C_3$ | $2.4584E-01$ | $8.9496E-01$ | $1.2812E+00$ | $2.6120E+00$ |
| $\alpha_3$ | $4.0672E-03$ | $2.6039E-01$ | $5.5443E-03$ | $2.6972E-01$ |
| $C_4$ | $1.7784E-01$ | $6.3240E-01$ | $1.4444E+00$ | $1.8188E+00$ |
| $\alpha_4$ | $1.2779E-01$ | $3.2351E-03$ | $1.0340E-01$ | $4.7116E-03$ |
| $C_5$ | 0 | $4.7301E-01$ | 0 | $1.4377E+00$ |
| $\alpha_5$ | 0 | $6.2658E-02$ | 0 | $7.2246E-02$ |
| $K_1$ | 0 | $3.9552E-04$ | $5.5417E-01$ | $3.4270E-03$ |
| $f_1$ | 0 | $1.0527E-01$ | $1.7904E-02$ | $1.2421E-01$ |
| $A_{r_1}$ | 0 | $1.3835E+00$ | $1.7813E+05$ | $1.9980E+00$ |
| $\varphi_1$ | 0 | $-1.9811E+00$ | $6.7820E-01$ | $1.4603E+00$ |
| $K_2$ | 0 | $3.2805E-02$ | $8.4039E-04$ | $2.4583E-03$ |
| $f_2$ | 0 | $4.4042E+00$ | $1.0384E-01$ | $2.2450E-01$ |
| $A_{r_2}$ | 0 | $2.4185E+00$ | $1.5521E+00$ | $1.5293E+00$ |
| $\varphi_2$ | 0 | $-6.6692E+00$ | $4.0532E+00$ | $-6.1765E+00$ |
| $K_3$ | 0 | 0 | $1.7842E-04$ | $6.4674E-04$ |
| $f_3$ | 0 | 0 | $1.7112E-01$ | $3.1642E-01$ |
| $A_{r_3}$ | 0 | 0 | $1.1211E+00$ | $1.1454E+00$ |
| $\varphi_3$ | 0 | 0 | $1.5805E+00$ | $1.7011E-01$ |
| $K_4$ | 0 | 0 | $6.6388E-02$ | $1.2479E-01$ |
| $f_4$ | 0 | 0 | $4.4591E+00$ | $4.5025E+00$ |
| $A_{r_4}$ | 0 | 0 | $2.2498E+00$ | $2.4045E+00$ |
| $\varphi_4$ | 0 | 0 | $-4.9733E-01$ | $-6.0588E-01$ |

TDS: time dial setting; $n$: number of fitted waveform components.

### *4.1. Case 1: GE IAC51 Relay*

Four characteristic curves corresponding to TDS 1, 4, 7, and 10 were selected for curve fitting and 486 sample points of relay operating time are taken for $M$ ranging from 1.5 to 50.0 with steps of 0.1. Table 1 lists the calculated mathematic parameters, where the selected number of fitted waveform components $n$ is the minimum number of waveform needed to construct the TDS curve. Equation (3.16) can be rewritten as (4.1) to represent the characteristic curves corresponding to the four TDS as

$$\begin{aligned} t(M) = {} & \sum_{i=1}^{5} C_i e^{-\alpha_i (M-1.4)} \\ & + 2\sum_{i=1}^{4} K_i A_{r_i}^{-f_i(M-1.4)} \cos\left(2\pi f_i (M-1.4) + \varphi_i\right). \end{aligned} \tag{4.1}$$

The number of the smooth waveform components $n_1$ was set to the maximum of the fitted result for the four TDS characteristic curves, and likewise for $n_2$ and $n_3$. The parameters of the waveform components not used in the fitted result were set to zero. This

**Table 2:** The curve-fitting errors of 17 actual operating times for each TDS of the IAC51 relay in milliseconds.

| TDS | 1 | | | 4 | | | 7 | | | 10 | | |
|---|---|---|---|---|---|---|---|---|---|---|---|---|
| $M$ | Top | SVD | Err | Top | SVD | Err | Top | SVD | Err | Top | SVD | Err |
| 1.5 | 1115.0 | 1112.6 | 2.34 | 4738.9 | 4738.9 | 0.02 | 9067.1 | 9067.1 | 0.01 | 14322.0 | 14322.0 | 0.16 |
| 2 | 753.7 | 756.8 | 3.11 | 3009.2 | 3011.1 | 1.87 | 5700.4 | 5702.3 | 1.89 | 8960.3 | 8964.3 | 3.99 |
| 3 | 530.5 | 529.2 | 1.31 | 2009.6 | 2008.3 | 1.30 | 3772.1 | 3770.0 | 2.05 | 5900.0 | 5896.7 | 3.25 |
| 4 | 442.2 | 443.4 | 1.15 | 1616.0 | 1616.3 | 0.32 | 3013.9 | 3014.0 | 0.10 | 4698.1 | 4697.7 | 0.49 |
| 6 | 362.4 | 361.8 | 0.61 | 1266.8 | 1266.2 | 0.59 | 2342.1 | 2340.9 | 1.22 | 3632.3 | 3631.1 | 1.21 |
| 8 | 323.3 | 322.4 | 0.82 | 1094.7 | 1094.4 | 0.34 | 2010.9 | 2010.4 | 0.48 | 3107.9 | 3106.7 | 1.18 |
| 10 | 298.2 | 298.6 | 0.47 | 985.7 | 986.2 | 0.48 | 1801.4 | 1802.0 | 0.66 | 2776.2 | 2778.1 | 1.92 |
| 13 | 275.0 | 275.2 | 0.22 | 881.8 | 881.9 | 0.12 | 1601.5 | 1601.3 | 0.29 | 2457.8 | 2455.8 | 2.04 |
| 16 | 259.3 | 259.3 | 0.04 | 812.5 | 812.8 | 0.34 | 1468.8 | 1469.2 | 0.42 | 2249.4 | 2250.6 | 1.25 |
| 19 | 247.4 | 247.6 | 0.20 | 763.2 | 763.1 | 0.04 | 1373.9 | 1373.6 | 0.28 | 2099.8 | 2099.0 | 0.84 |
| 22 | 239.5 | 238.9 | 0.66 | 726.4 | 726.2 | 0.18 | 1302.1 | 1302.0 | 0.12 | 1985.9 | 1984.6 | 1.29 |
| 26 | 230.6 | 230.1 | 0.49 | 686.3 | 686.7 | 0.46 | 1224.8 | 1226.1 | 1.36 | 1864.8 | 1865.8 | 1.06 |
| 30 | 223.7 | 223.4 | 0.21 | 655.8 | 655.8 | 0.08 | 1166.7 | 1166.5 | 0.18 | 1772.3 | 1773.0 | 0.66 |
| 34 | 217.4 | 218.1 | 0.66 | 630.5 | 630.8 | 0.29 | 1118.8 | 1119.1 | 0.24 | 1695.6 | 1696.3 | 0.67 |
| 39 | 211.6 | 212.4 | 0.88 | 604.8 | 604.7 | 0.11 | 1070.0 | 1069.4 | 0.66 | 1619.2 | 1619.0 | 0.15 |
| 44 | 207.1 | 207.5 | 0.41 | 583.8 | 583.9 | 0.08 | 1029.2 | 1029.4 | 0.20 | 1554.7 | 1553.9 | 0.88 |
| 49 | 202.9 | 203.0 | 0.09 | 566.3 | 566.1 | 0.26 | 994.7 | 994.3 | 0.38 | 1500.4 | 1499.8 | 0.64 |
| | | | AV = 0.80 | | | AV = 0.40 | | | AV = 0.62 | | | AV = 1.27 |

TDS: time dial setting; $M$: multiples of tap value current; top: actual operating time in milliseconds; SVD: fitted value by singular value decomposition; Err: absolute value of difference between top and SVD value; AV: average of absolute values of errors in milliseconds.

simple operating equation contains 26 parameters and includes $n_1 = 5$ smooth waveform components, $n_2 = 4$ paired oscillation waveform components and $n_3 - n_2 = 0$ unpaired oscillation waveform components. Since the minimum value of the samples of the multiples of tap value current of the characteristic curve is 1.5 and the sampling step $\Delta M = 0.1$, $\overline{M} = 1.5 - 0.1 = 1.4$.

Table 2 compares the 17 relay operating times and the corresponding SVD fitted values for each TDS. The average of absolute values of errors for each TDS is in the range 0.40–1.27 ms.

Table 3 summarizes the complete fitting results. The maximum absolute values of errors range from 3.62 to 8.73 ms, and all occur at smaller $M$ values (1.8, 2.2, 2.8, and 2.2). The maximum absolute values of percentage errors range from 0.15 to 0.48, and mostly occur in the smaller one-third of the range of $M$ (i.e., 41.4, 3.9, 3.9, and 12.1). The average of absolute values of errors range from 0.28 to 0.89 ms, and the average of absolute values of percentage errors ranges from 0.03 to 0.19.

Finally, Figure 3 shows the samples of the actual relay operating times and the corresponding values from the curve-fitting equations obtained by SVD. This figure shows that two sets of values are so closely matched that they are virtually indistinguishable. This clearly demonstrates the accuracy and identification robustness of the SVD method.

### *4.2. Case 2: ABB CO-8 Relay*

Four characteristic curves corresponding to TDS 0.5, 3, 6, and 9 were selected for curve fitting, and 488 sample points of relay operating time were taken for $M$ ranging from 1.3 to 50.0

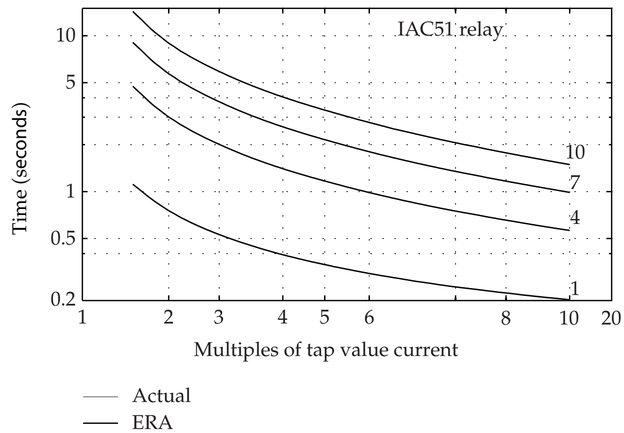


**Figure 3:** The actual characteristic curves and the curves fitted by (4.1) for the IAC51 relay.

**Table 3:** Summary of the SVD results for the IAC51 relay.

| TDS | Max_Err/$M$ | Max_Err%/$M$ | AV | AV% |
|---|---|---|---|---|
| 1 | 4.05/1.8 | 0.48/41.4 | 0.53 | 0.19 |
| 4 | 3.62/2.2 | 0.16/3.9 | 0.28 | 0.03 |
| 7 | 5.08/2.8 | 0.15/3.9 | 0.50 | 0.03 |
| 10 | 8.73/2.2 | 0.20/12.1 | 0.89 | 0.04 |

TDS: time dial setting; Max_Err/$M$: maximum absolute values of errors in millisecond in multiples of tap value current; Max_Err%/$M$: maximum absolute values of percentage errors in multiples of tap value current; AV: average of absolute values of errors in milliseconds; AV%: averages of absolute values of percentage errors.

with steps of 0.1. Table 4 lists the calculated mathematic parameters. Equation (3.16) can be rewritten as (4.2) to represent the characteristic curves corresponding to the four TDS as

$$t(M) = \sum_{i=1}^{6} C_i e^{-\alpha_i (M-1.2)} + 2\sum_{i=1}^{6} K_i A_{r_i}^{-f_i (M-1.2)} \cos\left(2\pi f_i (M-1.2) + \varphi_i\right) + K_7 A_{r_7}^{-f_7 (M-1.2)} \cos\left(2\pi f_7 (M-1.2) + \varphi_7\right). \tag{4.2}$$

This simple operating equation contains 40 parameters and includes $n_1 = 6$ smooth waveform components, $n_2 = 6$ paired oscillation waveform components, and $n_3 - n_2 = 1$ unpaired oscillation waveform components. Since the minimum value of the samples of the multiples of tap value current of the characteristic curve is 1.3 and the sampling step $\Delta M = 0.1$, $\overline{M} = 1.3 - 0.1 = 1.2$.

Table 5 compares the 17 relay operating times and the corresponding SVD fitted values for each TDS. The average of absolute values of errors for each TDS ranges from 0.37 to 0.95 ms.

Table 6 summarizes the complete fitting results. The maximum absolute values of errors range from 3.69 to 8.22 ms, and all occur at smaller $M$ values (i.e., 2.0, 3.9, 2.5, and 4.4).

**Table 4:** The 40 parameters in (4.2) for the CO-8 relay.

| TDS | 0.5 | 3 | 6 | 9 |
|---|---|---|---|---|
| $n$ | 9 | 12 | 15 | 19 |
| $C_1$ | $2.2260E+00$ | $2.5261E+01$ | $3.7055E+01$ | $5.8957E+01$ |
| $\alpha_1$ | $3.6161E+00$ | $3.7976E+00$ | $4.2328E+00$ | $3.5943E+00$ |
| $C_2$ | $9.4399E-01$ | $4.8815E-01$ | $2.3176E+01$ | $2.9885E+01$ |
| $\alpha_2$ | $9.7475E-01$ | $3.7793E-03$ | $1.8071E+00$ | $1.5467E+00$ |
| $C_3$ | $1.6429E-01$ | $5.1059E-01$ | $7.0000E+00$ | $9.1230E+00$ |
| $\alpha_3$ | $2.6196E-01$ | $1.1208E-01$ | $6.2423E-01$ | $6.0876E-01$ |
| $C_4$ | $2.3958E-02$ | $1.9846E+00$ | $1.0226E+00$ | $1.6539E+00$ |
| $\alpha_4$ | $-9.7055E-03$ | $4.1472E-01$ | $2.1111E-01$ | $2.3403E-01$ |
| $C_5$ | $5.1724E-02$ | 0 | $9.8116E-01$ | $1.5020E+00$ |
| $\alpha_5$ | $1.9268E-02$ | 0 | $3.4244E-03$ | $4.0665E-03$ |
| $C_6$ | 0 | 0 | $5.4251E-01$ | $1.0217E+00$ |
| $\alpha_6$ | 0 | 0 | $7.9622E-02$ | $7.9132E-02$ |
| $K_1$ | $1.2639E-04$ | $3.1088E+00$ | $3.7043E+00$ | $2.9481E-01$ |
| $f_1$ | $8.1404E-02$ | $6.7874E-02$ | $1.5581E+00$ | $1.0716E+00$ |
| $A_{r_1}$ | $1.5162E+00$ | $7.4100E+05$ | $5.2041E+02$ | $1.3713E+01$ |
| $\varphi_1$ | $-3.4533E-02$ | $1.6373E-01$ | $1.2089E+00$ | $-2.5188E+00$ |
| $K_2$ | $8.8486E-02$ | $2.3338E-02$ | $6.1002E-03$ | $4.7967E-03$ |
| $f_2$ | $3.3685E+00$ | $6.0254E-01$ | $2.8122E+00$ | $2.0997E+00$ |
| $A_{r_2}$ | $8.2508E+00$ | $4.8391E+00$ | $1.1917E+00$ | $1.1848E+00$ |
| $\varphi_2$ | $-1.7509E+00$ | $-2.5597E+00$ | $-7.5985E+00$ | $7.1928E-02$ |
| $K_3$ | 0 | $5.8643E+00$ | $2.1803E-02$ | $1.6860E-02$ |
| $f_3$ | 0 | $2.8484E+00$ | $3.3973E+00$ | $2.4543E+00$ |
| $A_{r_3}$ | 0 | $1.5179E+02$ | $1.3685E+00$ | $1.3082E+00$ |
| $\varphi_3$ | 0 | $-6.8235E+00$ | $3.3636E+00$ | $-1.1421E+00$ |
| $K_4$ | 0 | $1.5217E-01$ | $4.9041E-01$ | $3.8013E-02$ |
| $f_4$ | 0 | $4.3811E+00$ | $4.2044E+00$ | $2.8364E+00$ |
| $A_{r_4}$ | 0 | $1.7508E+00$ | $1.9500E+00$ | $1.3904E+00$ |
| $\varphi_4$ | 0 | $4.6268E-01$ | $-4.5837E+00$ | $-1.5897E+00$ |
| $K_5$ | 0 | 0 | 0 | $1.1831E-01$ |
| $f_5$ | 0 | 0 | 0 | $3.3797E+00$ |
| $A_{r_5}$ | 0 | 0 | 0 | $1.6111E+00$ |
| $\varphi_5$ | 0 | 0 | 0 | $-2.6524E+00$ |
| $K_6$ | 0 | 0 | 0 | $7.6744E-01$ |
| $f_6$ | 0 | 0 | 0 | $4.0923E+00$ |
| $A_{r_6}$ | 0 | 0 | 0 | $1.9734E+00$ |
| $\varphi_6$ | 0 | 0 | 0 | $-3.8092E+00$ |
| $K_7$ | 0 | 0 | $2.8143E+00$ | $2.9320E+00$ |
| $f_7$ | 0 | 0 | $5.0000E+00$ | $5.0000E+00$ |
| $A_{r_7}$ | 0 | 0 | $3.5972E+00$ | $2.7190E+00$ |
| $\varphi_7$ | 0 | 0 | $-3.1416E+00$ | $-3.1416E+00$ |

Please refer to Table 1 for the meanings of the terms.

The maximum absolute values of percentage errors ranges from 0.18 to 0.73, and also occur at smaller $M$ values. The average of absolute values of errors ranges from 0.17 to 0.58 ms, while the averages of absolute values of percentage errors ranges from 0.03 to 0.16.

**Table 5:** The curve-fitting errors of 17 actual operating times for each TDS of the CO-8 relay in milliseconds.

| TDS | 0.5 | | | 3 | | | 6 | | | 9 | | |
|---|---|---|---|---|---|---|---|---|---|---|---|---|
| $M$ | Top | SVD | Err | Top | SVD | Err | Top | SVD | Err | Top | SVD | Err |
| 1.5 | 1682.2 | 1682.1 | 0.11 | 15254.0 | 15254.0 | 0.10 | 31907.0 | 31907.0 | 0.26 | 50681.0 | 50681.0 | 0.16 |
| 2 | 760.5 | 764.2 | 3.69 | 6182.1 | 6182.6 | 0.49 | 13232.0 | 13232.0 | 0.21 | 21256.0 | 21257.0 | 1.11 |
| 3 | 343.9 | 343.6 | 0.25 | 2577.6 | 2581.6 | 3.98 | 5334.0 | 5337.1 | 3.10 | 8449.4 | 8450.2 | 0.78 |
| 4 | 213.7 | 214.3 | 0.60 | 1578.5 | 1578.0 | 0.44 | 3341.9 | 3339.4 | 2.51 | 5222.6 | 5218.7 | 3.92 |
| 6 | 128.1 | 127.6 | 0.55 | 1004.0 | 1002.7 | 1.24 | 2062.6 | 2060.3 | 2.32 | 3221.3 | 3218.3 | 3.02 |
| 8 | 99.7 | 99.7 | 0.01 | 821.3 | 820.2 | 1.12 | 1618.9 | 1618.4 | 0.44 | 2542.7 | 2540.0 | 2.66 |
| 10 | 86.1 | 86.3 | 0.19 | 711.7 | 712.9 | 1.13 | 1407.3 | 1409.4 | 2.16 | 2210.1 | 2211.9 | 1.79 |
| 13 | 75.8 | 75.7 | 0.04 | 618.3 | 617.9 | 0.42 | 1244.0 | 1243.5 | 0.56 | 1944.8 | 1944.7 | 0.10 |
| 16 | 70.1 | 70.0 | 0.10 | 563.1 | 563.1 | 0.01 | 1145.0 | 1145.3 | 0.30 | 1783.3 | 1783.9 | 0.62 |
| 19 | 66.5 | 66.6 | 0.13 | 526.5 | 527.1 | 0.56 | 1078.3 | 1078.6 | 0.28 | 1672.8 | 1672.7 | 0.06 |
| 22 | 64.7 | 64.6 | 0.07 | 501.4 | 501.2 | 0.12 | 1030.0 | 1029.9 | 0.06 | 1589.8 | 1589.9 | 0.13 |
| 26 | 62.9 | 62.9 | 0.01 | 476.0 | 476.2 | 0.23 | 982.0 | 982.0 | 0.02 | 1506.4 | 1506.5 | 0.02 |
| 30 | 61.4 | 61.4 | 0.00 | 458.5 | 458.1 | 0.47 | 946.5 | 946.1 | 0.36 | 1442.9 | 1442.6 | 0.33 |
| 34 | 60.1 | 60.4 | 0.35 | 443.7 | 444.2 | 0.45 | 917.4 | 917.8 | 0.38 | 1390.5 | 1391.4 | 0.93 |
| 39 | 59.6 | 59.6 | 0.02 | 430.7 | 430.6 | 0.19 | 889.1 | 889.1 | 0.02 | 1339.7 | 1339.5 | 0.14 |
| 44 | 59.0 | 58.9 | 0.09 | 419.3 | 419.5 | 0.20 | 865.5 | 865.5 | 0.03 | 1297.0 | 1296.7 | 0.27 |
| 49 | 58.6 | 58.7 | 0.12 | 409.8 | 409.9 | 0.11 | 845.0 | 845.1 | 0.14 | 1260.1 | 1259.9 | 0.15 |
| | | | AV = 0.37 | | | AV = 0.66 | | | AV = 0.77 | | | AV = 0.95 |

Please refer to Table 2 for the meanings of the terms.

**Table 6:** Summary of the SVD results for the CO-8 relay.

| TDS | Max_Err/$M$ | Max_Err%/$M$ | AV | AV% |
|---|---|---|---|---|
| 0.5 | 3.69/2.0 | 0.73/3.9 | 0.17 | 0.16 |
| 3 | 8.22/3.9 | 0.50/3.9 | 0.42 | 0.05 |
| 6 | 7.72/2.5 | 0.29/5.2 | 0.53 | 0.03 |
| 9 | 6.08/4.4 | 0.18/6.9 | 0.58 | 0.03 |

Please refer to Table 3 for the meanings of the terms.

The absolute values of error of 488 sample points with TDS 3 CO8 relay are shown in Figure 4. It can be seen that the absolute values of errors are within preset range, and the absolute values of errors at smaller values of $M$ are larger, in accordance with what was mentioned in Section 1 that, for EM OC relays, curve fitting is harder at small values of $M$ where the relay operating time changes nonlinearly and drastically.

Finally, Figure 5 shows the samples of the actual relay operating times and the corresponding values from the curve-fitting equations obtained by SVD. This figure shows that these two sets of values are also closely matched.

### *4.3. Result Analysis*

The following paragraphs analyze and compare the SVD fitting results for the IAC51 and CO-8 EM OC relays.

The maximum absolute values of errors of the hundreds of sample points calculated by SVD are within the millisecond range, which is accurate enough for practical purposes.

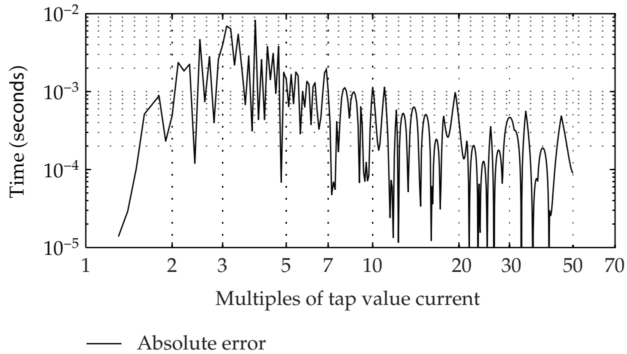


**Figure 4:** Absolute values of error for TDS = 3 CO-8 relay.

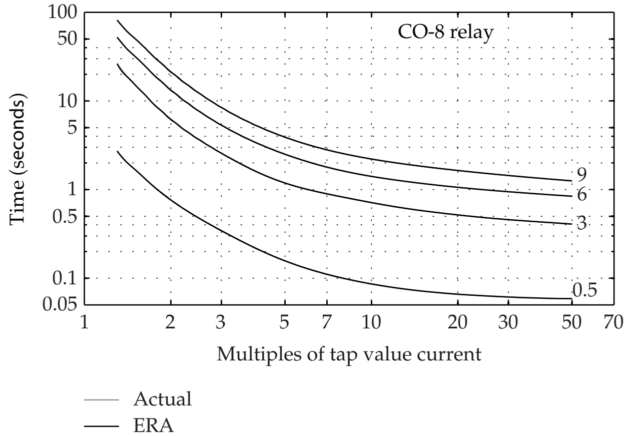


**Figure 5:** The actual characteristic curves and the curves fitted by (4.2) for the CO-8 relay.

However, more fitted waveform components can be selected if greater precision is desired. Although the maximum absolute values of errors and maximum absolute values of percentage errors primarily occur at small $M$ values where the relay operating time is highly nonlinear and changes rapidly, the curves fitted by SVD method still match the relay characteristic very well in the case study.

The SVD method can be applied to different types of inverse-time EM OC relay. As shown in Table 1 for the IAC51 relay, the numbers of fitted waveform components for the four characteristic curves with TDS 1, 4, 7, and 10 are 4, 9, 12, and 13, respectively. Table 4 shows the numbers of fitted waveform components for the four characteristic curves with TDS 0.5, 3, 6, and 9 are 9, 12, 15, and 19, respectively for the CO-8 relay. Relays with more inverse-time characteristics require more fitted waveform components to achieve the same range of maximum absolute values of errors. For a particular inverse-time EM OC relay, a larger number of fitted waveform components is also required to achieve the same range of maximum absolute values of errors for higher TDS. In any case, the fitted results for both types of relays are accurate enough for practical applications.

SVD can be applied to achieve excellent protection coordination between widely used digital relays and conventional EM OC relays. The procedures may be outlined below using CO-8 relay as an example, with a coordination time interval of 0.3 second.

*(a) Use the CO-8 Relay as the Primary Relay*

Set TDS = 5 so that $(t, M) = (1.098, 18)$. The setting of the backup digital relay should be $(t, M) = (1.398, 18)$ and can be easily accomplished by setting TDS = 6.49. This makes it easy to set the digital relay using the curve-fitted equation of the EM OC relay's characteristic curves with TDS = 6 and TDS = 7 as a base reference.

*(b) Use the Digital Relay to Achieve Adaptive Relay [1, 8] Protection Coordination*

First, apply SVD to determine the settings of the CO-8 relay and then calculate the operating time for the digital relay by adding 0.3 s to, or subtracting 0.3 s from, that of the CO-8 relay if the digital relay is to function as a backup or primary relay, respectively.

## 5. Comparison between SVD and ANFIS

In 2008, Geethanjali and Slochanal applied fuzzy logic and artificial neural network on six adaptive network and fuzzy inference system (ANFIS) algorithms (tri-mf5, gauss-mf5, gbell-mf5, tri-mf7, gauss-mf7, and gbell-mf7) for the characteristic curve fitting of one EM OC relay: the very inverse-time CRP9 relay with TDS = 4, 7, and 10 [9]. The current study applies the SVD method to the relay for the same TDS characteristic curves for comparison purposes, with sampling step 1.0, and 18 relay operating times [9]. Table 7 lists the calculated mathematic parameters. Equation (5.1) represents the characteristic curves as

$$\begin{aligned} t(M) = {} & \sum_{i=1}^{3} C_i e^{-\alpha_i (M-\overline{M})} \\ & + 2\sum_{i=1}^{3} K_i A_{r_i}^{-f_i(M-\overline{M})} \cos\left(2\pi f_i\left(M-\overline{M}\right)+\varphi_i\right) \\ & + \sum_{i=4}^{5} K_i A_{r_i}^{-f_i(M-\overline{M})} \cos\left(2\pi f_i\left(M-\overline{M}\right)+\varphi_i\right). \end{aligned} \tag{5.1}$$

This simple operating equation includes $n_1 = 3$ smooth waveform components, $n_2 = 3$ paired oscillation waveform components, and $n_3 - n_2 = 2$ unpaired oscillation waveform components. The minimum value of the samples of the multiples of tap value current of the characteristic curve is 3 for the CRP9 EM OC relay. Thus, the value of $\overline{M}$ is 2.

For each TDS, Table 8 compares the best results of each of the six ANFIS and those of SVD. For the CRP9 relay, the table shows that the ranges of maximum absolute values of errors are 0.00 ms and 16.00–28.00 ms, the ranges of maximum absolute values of percentage errors are 0.00 and 0.91–1.82, the ranges of averages of absolute values of errors are 0.00 ms and 5.20–11.80 ms and the ranges of averages of absolute values of percentage errors are 0.00 and 0.61–1.59, for the SVD and ANFIS, respectively.

Nine methods, which include the coefficient analytical model and fuzzy model in [7], SVD method and six ANFIS methods [9], are used to fit the same three TDS characteristic

**Table 7:** The 26 parameters in (5.1) for the CRP9 relay.

| TDS | 4 | 7 | 10 |
|---|---|---|---|
| $n$ | 9 | 9 | 9 |
| $C_1$ | $7.7404E + 00$ | $1.0543E + 03$ | $8.2698E + 02$ |
| $\alpha_1$ | $-1.6459E - 01$ | $2.6177E - 02$ | $-5.0138E - 03$ |
| $C_2$ | $9.5174E + 02$ | $2.2089E + 03$ | $2.3671E + 03$ |
| $\alpha_2$ | $8.3416E - 02$ | $3.5173E - 01$ | $1.6485E - 01$ |
| $C_3$ | $5.0011E + 03$ | $7.2570E + 03$ | $1.0160E + 04$ |
| $\alpha_3$ | $1.1198E + 00$ | $1.4926E + 00$ | $1.0356E + 00$ |
| $K_1$ | $6.9836E + 00$ | $1.1067E + 01$ | $5.1534E + 01$ |
| $f_1$ | $1.7548E - 01$ | $1.5364E - 01$ | $1.8441E - 01$ |
| $A_{r_1}$ | $1.7617E + 00$ | $1.2087E + 00$ | $2.6035E + 00$ |
| $\varphi_1$ | $-3.9473E + 00$ | $-2.8492E + 00$ | $-2.2634E + 00$ |
| $K_2$ | $3.3350E + 01$ | $2.4708E - 03$ | $3.9790E + 01$ |
| $f_2$ | $2.9238E - 01$ | $3.3275E - 01$ | $2.9308E - 01$ |
| $A_{r_2}$ | $3.4628E + 00$ | $2.8111E - 01$ | $2.2240E + 00$ |
| $\varphi_2$ | $9.8357E - 01$ | $2.2210E - 01$ | $-3.2530E + 00$ |
| $K_3$ | 0 | 0 | $3.8059E - 01$ |
| $f_3$ | 0 | 0 | $4.5246E - 01$ |
| $A_{r_3}$ | 0 | 0 | $7.3894E - 01$ |
| $\varphi_3$ | 0 | 0 | $-3.3901E + 00$ |
| $K_4$ | $1.4208E - 03$ | $5.0216E + 00$ | 0 |
| $f_4$ | $5.0000E - 01$ | $5.0000E - 01$ | 0 |
| $A_{r_4}$ | $4.6291E - 01$ | $1.0995E + 00$ | 0 |
| $\varphi_4$ | $-3.1416E + 00$ | $0.0000E + 00$ | 0 |
| $K_5$ | $1.3780E + 01$ | $5.2586E + 01$ | 0 |
| $f_5$ | $5.0000E - 01$ | $5.0000E - 01$ | 0 |
| $A_{r_5}$ | $2.0196E + 00$ | $2.8355E + 00$ | 0 |
| $\varphi_5$ | $-6.2832E + 00$ | $-3.1416E + 00$ | 0 |

Please refer to Table 1 for the meanings of the terms.

curves for CRP9 relay. The average values of absolute percentage errors are shown in Figure 6. SVD is clearly the best.

In summary, SVD outperforms ANFIS in curve fitting the operating time characteristics of the EM OC relay CRP9. Once again, this confirms the accuracy and identification robustness of the SVD method.

## 6. Conclusion

This study proposes an algorithm based on singular value decomposition (SVD) and fits the characteristic curves corresponding to eight TDS of two different types of inverse-time EM OC relays. The method decomposes the waveforms of the curves, according to their eigenvalues and corresponding eigenvectors, into various smooth and oscillating components without converting them to the frequency domain. Results show that the SVD performs exceedingly well in every respect regarding four different types of absolute values of errors. Although the maximum absolute values of errors and maximum absolute values of percentage errors primarily occur at small $M$ values where the relay operating time is highly

**Table 8:** Comparison of results by ANFIS and SVD for the CRP9 relay.

| $M$ | Top | ANFIS | Err1 | Err1% | SVD | Err | Err% |
|---|---|---|---|---|---|---|---|
| | | | | TDS = 4 | | | |
| 4 | 1352 | 1368 | 16 | 1.18 | 1352.00 | 0.00 | 0.00 |
| 8 | 605 | 609 | 4 | 0.66 | 605.00 | 0.00 | 0.00 |
| 12 | 459 | 456 | 3 | 0.65 | 459.00 | 0.00 | 0.00 |
| 16 | 375 | 374 | 1 | 0.27 | 375.00 | 0.00 | 0.00 |
| 20 | 358 | 356 | 2 | 0.56 | 358.00 | 0.00 | 0.00 |
| | | | AV = 5.2 | AV% = 1.59* | | AV = 0.00 | AV% = 0.00 |
| | | | | TDS = 7 | | | |
| 4 | 2459 | 2477 | 18 | 0.73 | 2459.00 | 0.00 | 0.00 |
| 8 | 1153 | 1132 | 21 | 1.82 | 1153.00 | 0.00 | 0.00 |
| 12 | 894 | 883 | 11 | 1.23 | 894.00 | 0.00 | 0.00 |
| 16 | 744 | 739 | 5 | 0.67 | 744.00 | 0.00 | 0.00 |
| 20 | 669 | 665 | 4 | 0.60 | 669.00 | 0.00 | 0.00 |
| | | | AV = 11.8 | AV% = 0.61* | | AV = 0.00 | AV% = 0.00 |
| | | | | TDS = 10 | | | |
| 4 | 3935 | 3963 | 28 | 0.71 | 3935.00 | 0.00 | 0.00 |
| 8 | 1754 | 1738 | 16 | 0.91 | 1754.00 | 0.00 | 0.00 |
| 12 | 1304 | 1305 | 1 | 0.08 | 1304.00 | 0.00 | 0.00 |
| 16 | 1123 | 1124 | 1 | 0.09 | 1123.00 | 0.00 | 0.00 |
| 20 | 1024 | 1027 | 3 | 0.29 | 1024.00 | 0.00 | 0.00 |
| | | | AV = 9.8 | AV% = 0.64* | | AV = 0.00 | AV% = 0.00 |

$M$: multiples of tap value current; TDS: time dial setting; top: actual operating time in milliseconds; ANFIS: fitted value by adaptive network and fuzzy inference system; Err1: absolute value of difference between top and ANFIS value; Err1%: absolute value of difference between top and ANFIS in percentage; SVD: fitted value by singular value decomposition; Err: absolute value of difference between top and SVD value; Err%: absolute value of difference between top and SVD value in percentage; AV: average of absolute values of errors in milliseconds; AV%: average of absolute values of percentage errors; *refer to [9].

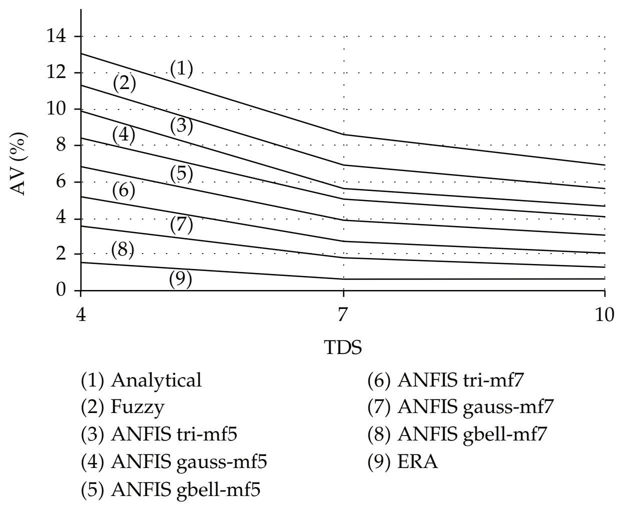


**Figure 6:** Average of absolute values of percentage errors of coefficient analytical model, fuzzy model, SVD method, and six ANFIS methods for CRP9 relay.

nonlinear and changes rapidly, the curves fitted by the SVD method can still match the relay characteristic very well. The SVD is also superior to ANFIS.

The ability to accurately represent the characteristic curves of the EM OC relays by a simple equation can provide good protection coordination between conventional EM OC relays and digital relays for subtransmission systems and distribution systems. The formula is a unified equation by SVD algorithm, and it can fit the characteristics of any piecewise nonlinear continuous smooth descending curves by simply changing the values of its parameters. Such convenience or advantage can be exploited not only for OC protection equipments such as EM OC relays or power fuses in power systems for practical applications or future studies, but also for any subject in any field with such characteristic.

## References

[1] A. Conde and E. Vazquez, "Application of a proposed overcurrent relay in radial distribution networks," *Electric Power Systems Research*, vol. 81, no. 2, pp. 570–579, 2011.

[2] M. S. Sachdev, J. Singh, and R. J. Fleming, "Mathematical models representing time-current characteristics of overcurrent relays for computer applications," in *Proceedings of the IEEE Power & Energy Society*, no. Paper No. A78-131-5, January 1978.

[3] IEEE Committee Report, "Computer representation of overcurrent relay characteristics," *IEEE Transactions on Power Delivery*, vol. 4, no. 3, pp. 1659–1667, 1989.

[4] S. Chan and R. Maurer, "Modeling overcurrent relay characteristics," *IEEE Computer Applications in Power*, vol. 5, no. 1, pp. 41–45, 1992.

[5] IEEE PSRC Committee, "IEEE standard inverse-time characteristic equations for overcurrent relays," *IEEE Transactoions on Power Delivery*, vol. 14, no. 3, pp. 868–872, 1999.

[6] D. J. Hill, L. W. Bruehler, and C. J. Bohrer, "Why wait? System-wide benefits from custom overcurrent relay characteristics," in *Proceedings of the 56th Annual Petroleum and Chemical Industry Conference (PCIC '09)*, pp. 1–9, September 2009.

[7] K. K. Hossein, A. A. Hossein, and A. D. Majid, "A flexible approach for overcurrent relay characteristics simulation," *Electric Power Systems Research*, vol. 66, no. 3, pp. 233–239, 2003.

[8] C. E. Arturo, V. M. Ernesto, and J. A. Héctor, "Time overcurrent adaptive relay," *International Journal of Electrical Power and Energy System*, vol. 25, no. 10, pp. 841–847, 2003.

[9] M. Geethanjali and S. M. R. Slochanal, "A combined adaptive network and fuzzy inference system (ANFIS) approach for overcurrent relay system," *Neurocomputing*, vol. 71, no. 4–6, pp. 895–903, 2008.

[10] H. A. Darwish, M. A. Rahman, A. I. Taalab, and H. Shaaban, "Digital model of overcurrent relay characteristics," in *Proceedings of the Conference Record of the IEEE Industry Applications 30th IAS Annual Meeting*, pp. 1187–1192, October 1995.

[11] B. Yan, X. Xie, and Q. Jiang, "Principal Hankel Component Algorithm (PHCA) for power system identification," in *Proceedings of the IEEE/PES Power Systems Conference and Exposition (PSCE '09)*, pp. 1–5, March 2009.

[12] J. S. H. Tsai, T. H. Chien, S. M. Guo, Y. P. Chang, and L. S. Shieh, "State-space self-tuning control for stochastic fractional-order chaotic systems," *IEEE Transactions on Circuits and Systems*, vol. 54, no. 3, pp. 632–642, 2007.

[13] S. M. Djouadi, R. C. Camphouse, and J. H. Myatt, "Reduced order models for boundary feedback flow control," in *Proceedings of the American Control Conference (ACC '08)*, pp. 4005–4010, June 2008.

[14] Z. Ma, S. Ahuja, and C. W. Rowley, "Reduced-order models for control of fluids using the eigensystem realization algorithm," *Theoretical and Computational Fluid Dynamics*, vol. 25, no. 1–4, pp. 233–247, 2011.

[15] X. D. Sun, T. Clarke, and M. A. Maiza, "A toolbox for minimal state space model realization," in *Proceedings of the IEE of Control Theory Application*, vol. 143, pp. 152–158, 1996.

[16] J. C. Tan, P. G. McLaren, R. P. Jayasinghe, and P. L. Wilson, "Software model for inverse time overcurrent relays incorporating IEC and IEEE standard curves," in *Proceedings of the IEEE Canadian Conference on Electrical and Computer Engineering*, vol. 1, pp. 37–41, May 2002.

[17] IEC Publication 255-3 (1989-05), Single input energizing quality measuring relays with dependent or independent.

[18] T. H. Tan and G. H. Tzeng, *Industry Power Distribution*, Gau Lih Book, 4th edition, 2011.

[19] BE1-1051 Manual, Basler Electric.

[20] J. N. Juang, *Applied System Identification*, Prentice Hall, Englewood Cliffs, NJ, USA, 1994.

[21] J. T. Kuan and M. K. Chen, "Parameter evaluation for lightning impulse with oscillation and overshoot using the eigensystem realization algorithm," *IEEE Transactions on Dielectrics and Electrical Insulation*, vol. 13, no. 6, pp. 1303–1316, 2006.

[22] Instructions GEK-49821F, *Phase Directional Overcurrent Relays*, General Electric, Ontario, Canada, 1999.


Advances in
Operations Research
Advances in
Decision Sciences
Journal of
Applied Mathematics
Algebra
Journal of
Probability and Statistics
The Scientific
World Journal
International Journal of
Differential Equations
Hindawi
Submit your manuscripts at
http://www.hindawi.com
International Journal of
Combinatorics
Advances in
Mathematical Physics
Journal of
Complex Analysis
Journal of
Mathematics
Mathematical Problems
in Engineering
Abstract and
Applied Analysis
Discrete Dynamics in
Nature and Society
International
Journal of
Mathematics and
Mathematical
Sciences
Journal of
Discrete Mathematics
Journal of
Function Spaces
International Journal of
Stochastic Analysis
Journal of
Optimization